

Domain-wall fermions and chiral symmetries

Sinya Aoki^a

^a Institute of Physics, University of Tsukuba, Tsukuba, Ibaraki 305-8571, Japan

We investigate chiral properties of the domain-wall fermion (DWF) system. After a brief introduction for the DWF, we summarize the recent numerical results on the chiral properties of the domain-wall QCD (DWQCD), which seem mutually inconsistent. We next derive a formula which connects a chiral symmetry breaking term in the five dimensional DWF Ward-Takahashi identity with the four-dimensional hermitian Wilson-Dirac operator. Based on this formula, we propose a solution, which resolves the inconsistency among recent numerical data, and give a consistent picture of the chiral properties of the DWQCD.

1. Introduction

A suitable definition of the chiral symmetry has been a long standing problem in lattice field theories. Recently an ultimate solution to this problem seems to appear in the form of the Ginsberg-Wilson relation [1,2]. Two explicit examples of the lattice fermion operators which satisfies the Ginsberg-Wilson relation have been found so far: One is the perfect lattice Dirac operator constructed via the renormalization group transformation[3] and the other is the overlap Dirac operator[4] derived from the overlap formalism[5] or from the domain-wall fermion(DWF)[6,7] in the limit of the infinite length of the 5th dimension. Since the explicit form is simpler for the latter, a lot of numerical investigations[8–11] as well as analytic considerations[12,13] have been carried out for the domain-wall fermion or the overlap Dirac fermion.

In this report we review the recent numerical investigations on the chiral properties of the DWF, which, however, bring puzzling results. To resolve these puzzles, we derive a formula which connects a chiral symmetry breaking term with the 4-dimensional hermitian Wilson-Dirac operator. Using this formula and the eigenvalue distribution of the Wilson-Dirac operator, we propose a consistent interpretation of puzzling results.

2. Domain-wall fermions

Throughout this report we employ a Shamir's variant of the original domain-wall fermion ac-

tion[7,?], which is equivalent to the 5-dimensional massive Wilson fermion with the free boundary condition in the 5-th direction, interacting with the 4-dimensional gauge field. Symbolically the action is given by

$$S_F = \bar{\psi} [\gamma^\mu D_\mu(A) + \gamma^5 \partial_5] \psi + \bar{\psi} [D_\mu(A)^2 + \partial_5^2] \psi + M \bar{\psi} \psi. \quad (1)$$

Note that the sign of the mass term M is opposite to the usual Wilson fermion. Since gauge fields are 4-dimensional, the 5-th coordinate s can be interpreted as “flavors”, so that the action can be rewritten in the 4-dimensional form:

$$S_F = \frac{1}{2} \bar{\psi}_{n,s} \gamma^\mu [U_{n,\mu} \psi_{n+\mu,s} - U_{n-\mu,\mu}^\dagger \psi_{n-\mu,s}] + \bar{\psi}_{n,s} [\mathcal{M}P_R + \mathcal{M}^\dagger P_L]_{s,t}^{n,m} \psi_{m,t}, \quad (2)$$

where the last term is considered as the flavor mixing “mass” term.

Now we consider the fermion spectrum derived from this action for the free theory. In this case the action in the momentum space becomes

$$S_F = \int d^4p [\bar{\psi}_s i \gamma^\mu \sin(p_\mu a) \psi_s + \bar{\psi}_s (\mathcal{M}P_R + \mathcal{M}^\dagger P_L)_{st} \psi_t] \quad (3)$$

where

$$\mathcal{M} = \begin{pmatrix} -W & 1 & & & \\ & -W & 1 & & \\ & & \ddots & \ddots & \\ & & & -W & 1 \\ & & & & -W \end{pmatrix}$$

Table 1
Relation between M and number of poles

condition	p_μ	# of poles
$0 < M < 2$	$(0, 0, 0, 0)$	1
$2 < M < 4$	$(\pi/a, 0, 0, 0)$	4
$4 < M < 6$	$(\pi/a, \pi/a, 0, 0)$	6
$6 < M < 8$	$(\pi/a, \pi/a, \pi/a, 0)$	4
$8 < M < 10$	$(\pi/a, \pi/a, \pi/a, \pi/a)$	1

$$\mathcal{M}^\dagger = \begin{pmatrix} -W & & & & & \\ 1 & -W & & & & \\ & & 1 & & & \\ & & & \ddots & & \\ & & & & \ddots & -W \\ & & & & & 1 & -W \end{pmatrix}$$

with $W = 1 - M + \sum_\mu [1 - \cos(p_\mu a)]$.

By setting $\psi(p)_s = P_R u_R(p)_s + P_L u_L(p)_s$, one observe that the solution to the equation $\mathcal{M}_{st} u_R(p)_t = 0$ ($\mathcal{M}_{st}^\dagger u_L(p)_t = 0$) gives a right-handed (left-handed) zero mode. The solutions to these equations are given by

$$u_R(p)_s = W(p)^{s-1} c_R \quad (4)$$

$$u_L(p)_s = W(p)^{N_s-s} c_L, \quad (5)$$

where N_s is the number of sites in the 5-th dimension. In order to satisfy the boundary conditions

$$u_R(N_s) = W(p)^{N_s-1} c_R = 0 \quad (6)$$

$$u_L(1) = W(p)^{N_s-1} c_L = 0 \quad (7)$$

for the above solutions, the $N_s \rightarrow \infty$ limit is necessary, together with the condition that $|W(p)| < 1$, which is equivalent to

$$0 < M + \sum_\mu (\cos(p_\mu a) - 1) < 2. \quad (8)$$

Since we have the kinetic term $\gamma^\mu \sin(p_\mu a)$ for the fermion, the condition that $p_\mu a \simeq 0$ or π is required for the existence of the massless pole in the continuum limit. Eq.(8) gives a condition for M and p_μ , which is summarized in table 1. It is clear that the value of M (Wilson fermion mass) controls the number of massless fermion poles. For $0 < M < 2$ we have one physical massless Dirac fermion.

The form of zero-modes obtained above is too complicated in the coordinate space even for the

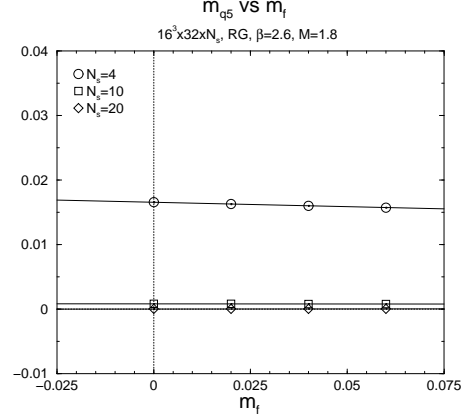


Figure 1. m_{q5} as a function of m_f on a $16^3 \times 32 \times N_s$ ($N_s = 4, 10$ and 20) at $M = 1.8$ and $\beta = 2.6$ for the renormalization group (RG) improved gauge action.

free theory to define the quark field as $P_R u_R + P_L u_L$. Instead we define the quark field as

$$q_n \equiv P_R \psi_{n,1} + P_L \psi_{n,N_s} \quad (9)$$

$$\bar{q}_n \equiv \bar{\psi}_{n,1} P_L + \bar{\psi}_{n,N_s} P_R. \quad (10)$$

This definition is reasonable since the right-handed zero mode has a peak at $s = 1$ and the left-handed one at $s = N_s$.

According to this definition, the quark mass term is given by $-m_f \bar{q}_n q_n$, which leads to the non-zero pole mass of the fermion for $0 < M < 2$:

$$m_{\text{pole}} = M(2 - M)[m_f + (1 - M)^{N_s}]. \quad (11)$$

The formula tells us that $m_{\text{pole}} \sim (1 - M)^{N_s} \neq 0$ even at $m_f = 0$ for $N_s \neq \infty$, corresponding to the fact that no solution to zero modes exist for finite N_s . On the other hand the fact that $m_{\text{pole}} \propto m_f$ in the $N_s \rightarrow \infty$ limit strongly suggests that the chiral symmetry is realized for the DWF. The lattice QCD with the DWF is called the domain-wall QCD (DWQCD).

As suggested by the behavior of the pole mass, the DWQCD satisfies the almost exact axial Ward-Takahashi identity, which is given by

$$\langle \{ \Delta_4 A_4^b(t) + 2m_f \bar{q} \gamma_5 \tau^b q(t) - 2j_5^b(t, N_s/2) \} \mathcal{O} \rangle + \langle \delta_t^b \mathcal{O} \rangle = 0 \quad (12)$$

where A_4^b is an axial-vector current, \mathcal{O} is an arbitrary operators which contain q and \bar{q} only as

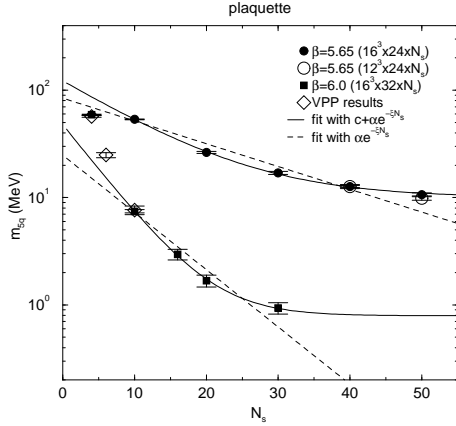


Figure 2. m_{q5} as a function of N_s for the plaquette gauge action at $a \simeq 0.2$ fm(circles) and 0.1 fm(squares).

the fermion variable, and $j_5^b(t, N_s/2)$, defined in the middle of the 5-th dimension, represents the explicit breaking term of the chiral symmetry.

In perturbation theory it is proven that $\langle j_5^b(t, N_s/2)\mathcal{O} \rangle \rightarrow 0$ as $N_s \rightarrow \infty$ for the non-singlet sector ($b \neq 0$), while $\langle j_5^b(t, N_s/2)\mathcal{O} \rangle \propto F_{\mu\nu}\tilde{F}_{\mu\nu} \neq 0$ for the singlet sector ($b = 0$). The latter one corresponds to the $U_A(1)$ anomaly, well-known in the continuum QCD.

Again the presence of the exact axial Ward-Takahashi in the DWQCD suggests the existence of the chiral symmetry in the $N_s \rightarrow \infty$ limit even for interacting theories.

3. Numerical investigation of chiral properties of the DWQCD

In order to investigate the chiral properties of the DWQCD, we define the anomalous quark mass in axial Ward-Takahashi identity as follows.

$$m_{q5} = \lim_{t \rightarrow \infty} \frac{\langle j_5^a(t, N_s/2) \cdot \bar{q}\gamma_5\tau^a q(0) \rangle}{\langle \bar{q}\gamma_5\tau^a q(t) \cdot \bar{q}\gamma_5\tau^a q(0) \rangle} \quad (13)$$

We expect that m_{q5} behaves as

$$m_{q5} = C + \alpha \exp[-\xi N_s] + \gamma m_f + O(m_f^2). \quad (14)$$

The existence of the massless fermion requires $C = 0$.

In Fig. 1, we have plotted m_{q5} as a function of m_f with $M = 1.8$ on a $L^3 \times T \times N_s = 16^3 \times 32 \times (4, 10, 20)$ lattice at $\beta = 2.6$ of the

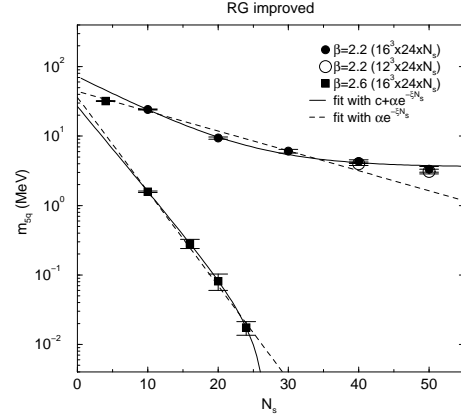


Figure 3. Same as Fig.2 for the RG improved gauge action.

renormalization group (RG) improved gauge action [11].

The figure shows that m_f dependence of m_{q5} is much milder than that of m_π^2 and is almost constant, so that the extrapolation of m_{q5} to $m_f = 0$ becomes much easier. In addition m_{q5} is very precise and sensitive to N_s , so that the N_s dependence can be extracted. Hereafter we exclusively employ m_{q5} to investigate the chiral properties of the DWQCD, because of these advantages of m_{q5} .

We have plotted m_{q5} as a function of N_s , calculated on the CP-PACS for the plaquette gauge action in Fig.2 and the RG improved gauge action(lower) in Fig.3, at coarse($a \simeq 0.2$ fm) and fine($a \simeq 0.1$ fm) lattice spacings[11].

At both lattice spacings m_{q5} is smaller for the RG improved action than for the plaquette action. At the coarse lattice spacing($a \simeq 0.2$ fm) it seems that $C \neq 0$ for both actions. On the other hand, $C = 0$ for the RG action while $C \neq 0$ for the plaquette action at the fine lattice spacing ($a \simeq 0.1$ fm).

4. Phase structure of the Wilson fermion and the DWQCD

In this section we try to understand the dependences of m_{q5} on the lattice spacings and the gauge actions. The existence of massless fermion of the DWQCD can be proven in the absence of zero eigenvalues of the hermitian Wilson-Dirac operator $H_W = \gamma_5 D_W(M)$, where $D_W(M)$ is the

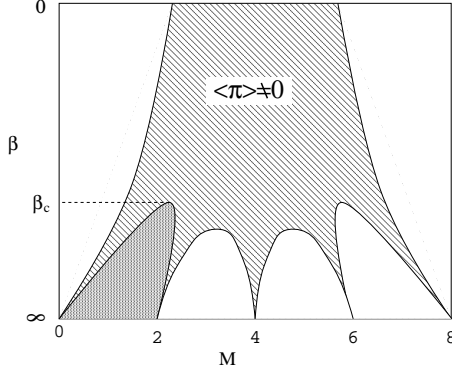


Figure 4. The expected phase structure of the lattice QCD with the Wilson fermion in the $\beta = 6/g^2 - M$ plane, where $\pi = \bar{q}i\gamma_5\tau^3q$.

4-dimensional Wilson fermion operator with the fermion mass M and $D_W(M)^\dagger = \gamma_5 D_W(M) \gamma_5$ is satisfied.

In the case of the 4-dimensional Wilson fermion, zero eigenvalues of $\gamma_5 D_W$ leads to the spontaneous breaking of parity-flavor symmetries, $\langle \bar{q}i\gamma_5\tau^3q \rangle \neq 0$, as shown below[14].

$$\begin{aligned}
 \langle \bar{q}i\gamma_5\tau^3q \rangle &= - \lim_{H \rightarrow +0} \text{Tr} \frac{i\gamma_5\tau^3}{D_W + i\gamma_5\tau^3H} \\
 &= - \lim_{H \rightarrow +0} \text{tr} \left[\frac{i\gamma_5}{D_W + i\gamma_5H} - \frac{i\gamma_5}{D_W - i\gamma_5H} \right] \\
 &= -i \lim_{H \rightarrow +0} \text{tr} \left[\frac{1}{H_W + iH} - \frac{1}{H_W - iH} \right] \\
 &= -i \lim_{H \rightarrow +0} \sum_n \left\langle \lambda_n \left| \left(\frac{1}{\lambda_n + iH} - \frac{1}{\lambda_n - iH} \right) \right| \lambda_n \right\rangle \\
 &= -i \lim_{H \rightarrow +0} \int d\lambda \rho_{H_W}(\lambda) \left\langle \lambda \left| \left(\frac{1}{\lambda + iH} - \frac{1}{\lambda - iH} \right) \right| \lambda \right\rangle \\
 &= -i \int d\lambda \rho_{H_W}(\lambda) (-2\pi i) \delta(\lambda) \\
 &= -2\pi \rho_{H_W}(0)
 \end{aligned}$$

where $\rho_{H_W}(\lambda)$ is the density of the eigenvalues of H_W , which is defined by

$$\rho_{H_W}(\lambda) = \sum_n \delta(\lambda_n - \lambda).$$

In Fig.4, we have drawn the expected phase structure of the lattice QCD with the Wilson fermion in the $\beta = 6/g^2 - M$ plane, where g^2 is the

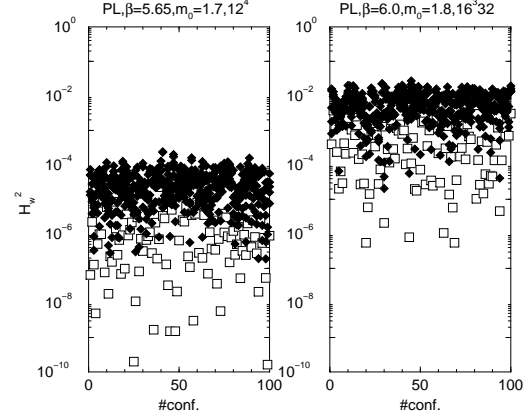


Figure 5. Monte Carlo time histories for the lowest six eigenvalues of H_W^2 obtained with the plaquette gauge action.

gauge coupling constant[14]. The small value of β corresponds to the coarse lattice spacing while the large value to the fine lattice. At $g^2 = 0$ ($\beta = \infty$) no zero eigenvalues exist for $0 < M < 2$, which is the region where the domain-wall fermion has the zero modes. If we increase the gauge coupling, the allowed region of M for the massless DWF becomes narrow and is shifted to larger values of M . Finally the allowed region disappears at $\beta = \beta_c$. This implies that massless fermions disappear at $\beta < \beta_c$ for the (quenched) DWQCD.

According to this interpretation it seems that $\beta_c > 5.65$ ($a = 0.2$ fm), 6.0 ($a = 0.1$ fm) for the plaquette gauge action, while the numerical data indicate that 2.6 ($a = 0.1$ fm) $> \beta_c > 2.2$ ($a = 0.2$ fm) for the RG improved gauge action.

5. Eigenvalues of H_W and $\rho_{H_W}(0)$

In this section we directly investigate the distribution of small eigenvalues of H_W .

In Figs. 5 and 6 we plot Monte Carlo time histories for the lowest six eigenvalues of H_W^2 for the plaquette and RG-improved actions[16]. The figures at $a \simeq 0.1$ fm are shown at the same lattice size with the previous work of m_{5q} . In each figure the left panel shows results for $a \simeq 0.2$ fm and the right panel for $a \simeq 0.1$ fm. Open squares show the minimum eigenvalue λ_{\min}^2 and filled diamonds

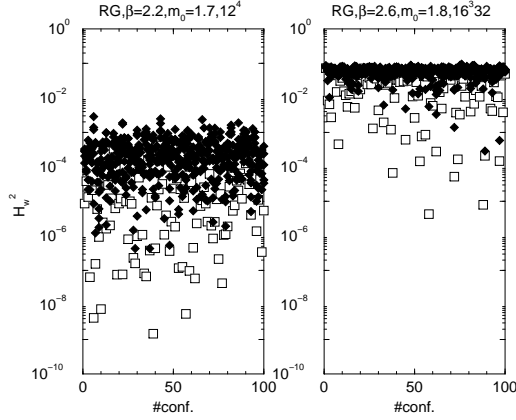


Figure 6. The same as Fig. 5 obtained with the RG-improved gauge action.

are the higher five eigenvalues.

There is a clear trend that the minimum eigenvalues become larger for smaller lattice spacings. Another interesting point is that the RG-improved action gives larger values λ_{\min}^2 than the plaquette action, which indicates that the RG-improved action has a better chiral behavior.

The spectral density of H_W is defined by

$$\rho_{H_W}(\lambda) = \lim_{V \rightarrow \infty} \frac{1}{3 \cdot 4 \cdot V} \sum_{\lambda'} \delta(\lambda' - \lambda), \quad (16)$$

where the summation is over the eigenvalues of H_W . The density of zero-eigenvalues $\rho_{H_W}(0)$, related to the order parameter of the parity-flavor breaking, has been calculated by the accumulation method proposed in [15], which is based on the relation

$$\begin{aligned} \frac{1}{3 \cdot 4 \cdot V} \sum_{|\lambda'| \leq \lambda} \mathbf{1} &= \int_{-\lambda}^{\lambda} d\lambda' \rho(\lambda') \\ &\simeq 2\rho(0)\lambda + O(\lambda^2). \end{aligned} \quad (17)$$

We note that, for the small- λ expansion in (17), analyticity of $\rho(\lambda)$ at the origin is assumed.

The result of [15], where $\rho_{H_W}(0)$ at several β 's have been plotted as a function of M , is given in Fig. 7 for the plaquette gauge action. Although $\rho_{H_W}(0)$ becomes smaller for smaller a (; larger β), no region without zero eigenvalues seems to exist. This impression is indeed confirmed in Fig. 8,

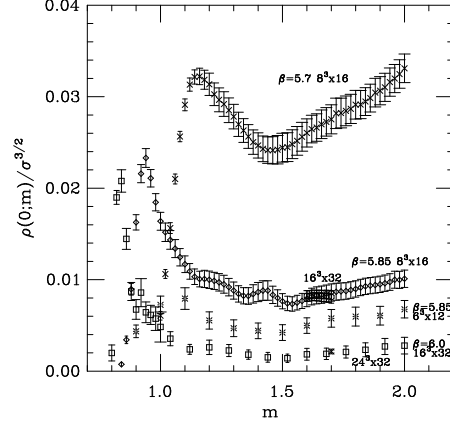


Figure 7. $\rho_{H_W}(0)$ as a function of M at several values of β for the plaquette action[15].

where $\rho_{H_W}(0)$ has been plotted as a function of $a^{-1/2}$ at $M = 1.2$ [15].

It has been speculated in [?] that the a dependence of $\rho_{H_W}(0)$ is well reproduced by the form that

$$\rho_{H_W}(0) \simeq A \exp\left[-\frac{c}{\sqrt{a}}\right]. \quad (18)$$

If this form is correct for all M , the region with $\rho_{H_W}(0) = 0$ does not exist as long as $a \neq 0$. The similar result has been obtained for the RG improved action.

These results immediately lead to the conclusion that there is no gap of the parity-flavor breaking phase in the g^2 - M plane for the Wilson fermion, so that the domain-wall QCD fails to realize the chiral symmetry at all $a \neq 0$. However this conclusion seems to contradict the numerical data for the RG improved gauge action at $a = 0.1$ fm. Puzzles still remain.

6. Theoretical understanding for the behavior of m_{q5}

In this section we try to understand the pathological behavior of m_{q5} as a function of N_s , in terms of the eigenvalues of H_W .

We first derive the analytic expression for m_{q5} as follows.

$$\frac{2m_{q5}a_5}{(1 - m_f)^2} = \frac{\sum_{X,Y} |\langle X | f(\tilde{H})^{-1} H_{GW}^{-1} | Y \rangle|^2}{\sum_{X,Y} |\langle X | H_{GW}^{-1} | Y \rangle|^2} \quad (19)$$

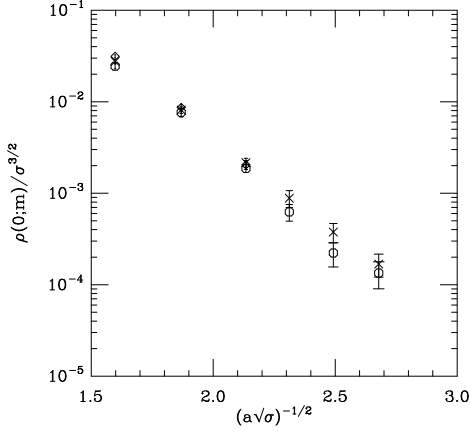


Figure 8. $\rho_{H_W}(0)$ as a function of $a^{-1/2}$ at $M = 1.2$ for the plaquette action[15].

where $X = (x, \alpha, a)$ represents site, spinor and color indices,

$$\begin{aligned}
 f(\tilde{H}) &= \cosh(\tilde{H}N_s/2) = \frac{T^{-N_s/2} + T^{N_s/2}}{2} \\
 T &= \frac{1 - H'_W}{1 + H'_W} \\
 H'_W &= H_W \frac{1}{2 + \gamma_5 H_W} \\
 H_{GW}^{-1} &= \frac{1}{(1 + m_f) + (1 - m_f)\gamma_5 \tanh(\tilde{H}N_s/2)} \gamma_5
 \end{aligned}$$

For the derivation of the above formula, see [17].

Based on the above formula m_{q_5} can be approximately estimated at $m_f = 0$ as follows.

$$\begin{aligned}
 2m_{q_5}a_5 &= \frac{1}{N_{all}} \left[c_0 \sum_{n=1}^{N_D} f(\tilde{\lambda}_n)^{-2} \right. \\
 &\quad \left. + (N_{all} - N_D) \int d\lambda \rho(\lambda) f(\tilde{\lambda})^{-2} \right] \\
 &= \frac{1}{N_{all}} \left[c_0 \sum_n f(\tilde{\lambda}_n)^{-2} + \sum_c f(\tilde{\lambda}_c)^{-2} \right] \quad (20) \\
 \tilde{\lambda} &= \log \frac{1 - \lambda}{1 + \lambda} \quad (21)
 \end{aligned}$$

where $\lambda_c(\lambda_n)$ is the continuous(discrete) eigenvalue of H'_W , N_D is the number of discrete modes, $N_{all} = L^3 \times T \times N_c \times 4$ is the number of degrees of freedom, and c_0 is a weight factor for the discrete modes. See [17] for the detail of the estimation.

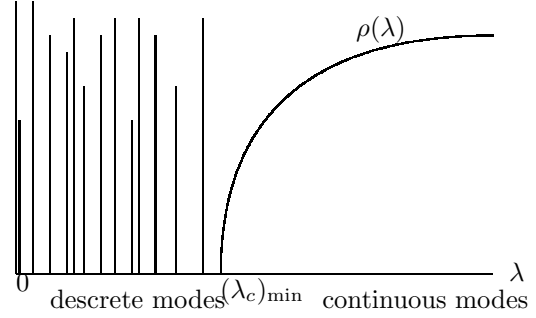


Figure 9. The expected distribution of the eigenvalues of \tilde{H}_W in the weak coupling region.

The important point is that there are two types of eigenvalues, the continuous eigenvalues and the discrete eigenvalues. The eigenfunction for the former is the plain-wave like and spreads over whole space, while the one for the latter is exponentially localized. In the strong coupling region at $\beta < \beta_c$, the continuous eigenvalues can become zero, so that $\rho_{H_W}(0) \neq 0$. Therefore the DWQCD does not work as expected. (See [?] for more details.) In the weak coupling region, on the other hand, the continuous eigenvalues has a minimum value $(\lambda_c)_{min}$, such that $\rho_{H_W}(\lambda_c < (\lambda_c)_{min}) = 0$ for the continuous eigenvalues. Instead of the continuous eigenvalues, discrete eigenvalues may become almost zero. The expected distribution of eigenvalues λ in the weak coupling region is schematically drawn in Fig. 9.

It is likely that small (localized) discrete eigenvalues are caused by dislocations. In particular, Q , the value of the topological charge in some configuration should move to the different value Q' during the simulation of the lattice QCD, so that the dislocation appears during the transition from Q to Q' . If the dislocation appears, the Wilson-Dirac operator has an almost zero eigenvalue at some value of M . Therefore it is very difficult to avoid small (localized) eigenvalues of H_W and \tilde{H}_W .

From the approximated estimate for m_{q_5} , only near zero eigenvalues can contribute to it as $N_s \rightarrow \infty$. Hence only small discrete eigenvalues are dangerous for the DWQCD in the weak coupling region. The analysis in [17] leads to the followings.

In the $N_s \rightarrow \infty$ limit m_{q_5} vanish at finite vol-

ume ($;N_{all} \neq \infty$), since the probability of having exact zero eigenvalues is zero.

If the infinite volume ($;N_{all} \rightarrow \infty$) limit is taken before the $N_s \rightarrow \infty$ limit, there are two possibilities for the distribution of discrete eigenvalues. Unless the number of near zero eigenvalues increases linearly in N_{all} , they does not contribute to m_{q5} , hence the DWQCD works fine. If it increases linearly in N_{all} , $\rho_{H_W}(0)$ and hence m_{q5} becomes non-zero, so that the DWQCD can not realize the chiral symmetry.

The numerical data obtained so far seem to prefer the latter possibility. However more detailed investigations will be necessary for the definite conclusion.

7. Conclusion

The distribution of near zero eigenvalues of H_W plays a crucial role for the chiral properties of the DWQCD. We have pointed out that there are two types of eigenvalues, continuous and discrete. In the weak coupling region, only discrete eigenvalues become relevant for m_{q5} . However the effect of discrete eigenvalues to m_{q5} is rather small even if the number of near zero discrete eigenvalues increases linearly in the volume. We think that this has brought confusing numerical results for the N_s dependence of m_{q5} .

Our analysis suggests that the gap is closed in the phase structure of the Wilson fermion due to the near zero discrete eigenvalues, if the quenched approximation is employed. In the dynamical QCD simulation, the near zero discrete eigenvalues are strongly suppressed by the fermion determinant, so that the gap opens and the expected phase structure is correct in the real lattice QCD. Since such a suppression of small discrete eigenvalues is not known for the DWQCD, it is unclear how the dynamical DWQCD change the distribution of the near zero discrete eigenvalues.

Acknowledgments

I would like to thank Dr. Y. Taniguchi, with whom I have completed the main part of this work. I also thank the members of the CP-PACS collaboration for some results presented in this re-

port, and Prof. H. Neuberger for the useful discussion. This work is supported in part by Grants-in-Aid of the Ministry of Education(No. 12640253).

REFERENCES

1. P. Ginsparg and K. Wilson, Phys. Rev. D25, 2649 (1982).
2. M. Lüscher, Phys. Lett. B428, 342 (1998).
3. P. Hasenfratz, Nucl. Phys. B525, 401 (1998); P. Hasenfratz, V. Laliena and F. Niedermayer, Phys. Lett. B427, 125 (1998).
4. H. Neuberger, Phys. Lett. B417, 141 (1998); Phys. Lett. B427, 353 (1998); Phys. Rev. D57, 5417 (1998).
5. R. Narayanan and H. Neuberger, Nucl. Phys. B412, 574 (1994); Nucl. Phys. B443, 305 (1995).
6. D. Kaplan, Phys. Lett. B288, 342 (1992).
7. Y. Shamir, Nucl. Phys. B406, 90 (1993); V. Furman and Y. Shamir, Nucl. Phys. B439, 54 (1995).
8. T. Blum and A. Soni, Phys. Rev. D56, 174 (1997); Phys. Rev. Lett. 79, 3595 (1997); hep-lat/9712004.
9. S. Aoki, T. Izubuchi, Y. Kuramashi and Y. Taniguchi, Phys. Rev. D62, 094502 (2000).
10. For a review, see T. Blum, Nucl. Phys. B (Proc. Suppl.) 73, 167 (1999) and references there in.
11. CP-PACS Collaboration, A. Ali Khan *et al.*, Phys. Rev. D63, 114504 (2001); Nucl. Phys. B (Proc. Suppl.) 83-84, 591 (2000).
12. P. Hernandez, K. Jansen and M. Lüscher, Nucl. Phys. B552, 363 (1999).
13. Y. Kikukawa, Nucl. Phys. B584, 511 (2000); Y. Kikukawa and T. Noguchi, hep-lat/9902022.
14. S. Aoki, Phys. Rev. D30, 2653 (1984); Phys. Rev. Lett. 57, 3136 (1986); Nucl. Phys. B314, 79 (1989).
15. R. Edwards, U. Heller and R. Narayanan, Phys. Rev. D60, 1999 (034502).
16. CP-PACS Collaboration, A. Ali Khan *et al.*, Nucl. Phys. B (Proc. Suppl.) 94, 725 (2001)
17. S. Aoki and Y. Taniguchi, hep-lat/0109022.